Journal of Engineering Research and Reports

Volume 24, Issue 11, Page 20-26, 2023; Article no.JERR.98153
ISSN: 2582-2926

Finite Element Simulation Analysis of Central Pull-out Experiment of Steel Bar and Recycled Concrete

Qianli Liu [a], Qian Zhu [a*], Ruiying Zhao [a], Xuejiao Chen [a], Jianzhuang Qi [a] and Tan Yao [a]

[a] *School of Civil Engineering and Architecture, Zhengzhou University of Aeronautics, Zhengzhou-450046, China.*

Authors' contributions

This work was carried out in collaboration among all authors. All authors read and approved the final manuscript.

Article Information

DOI: 10.9734/JERR/2023/v24i11851

Open Peer Review History:
This journal follows the Advanced Open Peer Review policy. Identity of the Reviewers, Editor(s) and additional Reviewers, peer review comments, different versions of the manuscript, comments of the editors, etc are available here: https://www.sdiarticle5.com/review-history/98153

Original Research Article

Received: 28/01/2023
Accepted: 30/03/2023
Published: 04/04/2023

ABSTRACT

In order to study the bond performance of steel bars and recycled concrete, the ultimate bond stress distribution between recycled concrete and steel bars is analyzed through central pull-out test, and the influence of steel bars grooving on actual stress distribution is considered. Therefore, in this paper uses the finite element software ABAQUS is used to simulate the central pull-out test of steel bars and recycled concrete, and to discuss the bond force distribution between steel bars and concrete. The results show that the finite element simulation analysis results of the central pull-out experiment of steel bars and recycled concrete are in good agreement with the experimental results, which verifies the accuracy of the finite element model.

Keywords: Recycled concrete; center pull out experiment; finite element model; simulation analysis.

**Corresponding author: Email: zhuqian@zua.edu.cn;*

1. INTRODUCTION

With the development of the construction industry, construction waste is increasing daily, which brings serious environmental pollution and waste of resources. The emergence of recycled concrete not only solves the above problems but also saves a lot of aggregate natural resources. In order to ensure that the steel bar and concrete can bear the force together, it is necessary to have a reliable bond strength between the steel bar and the concrete. Due to a large amount of cement mortar attached to the surface of the recycled aggregate, the bonding performance between the steel bar and the recycled concrete is different from that of ordinary concrete. Therefore, in-depth research on the anchorage of recycled concrete reinforcement is of great significance [1].

Regarding the bonding performance of recycled aggregate reinforced concrete, relevant research has been carried out at home and abroad [2-8], but generally, qualitative or macroscopic studies are conducted through simple pull-out tests, and what is obtained is only the average value converted from the pull-out force. It cannot fundamentally reveal the distribution law of the bond force between steel bars and concrete [9]. In addition, to measure the bonding performance of recycled concrete, it is necessary to know the strain change of the steel bars in the specimen, which is difficult to measure by conventional means. If the built-in strain gauge method is used to test the strain, not only the slotting will affect the actual stress distribution of the steel bar. Moreover, due to the influence of various factors in the test, the results have large errors.

Therefore, with the help of finite element simulation and test, this paper reveals the law of the distribution of bond force between recycled aggregate concrete and steel bars and provides powerful evidence for explaining the bond force distribution of reinforced concrete fundamentally.

2. EXPERIMENTAL PROCEDURE

2.1 Test Piece Design and Production

The sample is a cube with a side length of 150mm. The steel bar at the unbonded part of the concrete at both ends of the test piece is covered with a 50mm long rigid PVC sleeve, and the gap between the end of the sleeve and the steel bar is closed. To measure the transfer of steel stress in concrete, a steel bar gauge is embedded in the concrete to measure the strain of the concrete, and the end face of the steel bar is processed into a smooth surface perpendicular to the bar axis to install the dial indicator.

The cement used in this test is ordinary Portland cement with P O 42.5 and natural river sand with a fineness modulus of 2.8. The aggregates are natural coarse aggregate NCA and recycled coarse aggregate RCA, where RCA is taken from abandoned C40 concrete beams, NCA is taken from crushed limestone, and the basic physical indicators of the coarse aggregate meet the requirements of GB/T 14685-2011 《Pebbles and Crushed Stones for Construction》; and GB/T 25177-2010 《 Recycled Coarse Aggregate for Concrete》. The water-reducing rate of high-efficiency water-reducing agents is 25%. The steel bars are HRB400 ribbed bars with a diameter of 8 mm.

2.2 Test Methods

The schematic diagram of the test loading device is shown in Fig. 1. Two displacement sensors are installed at the loading end and the free end of the specimen, respectively, to measure the slippage of the steel bar at the loading end and the free end relative to the specimen. The bonding test is loaded on a 100t universal testing machine using displacement control, with a loading rate of 0.3 mm/min. The DH3818Y static signal acquisition and analysis system is used for data acquisition.

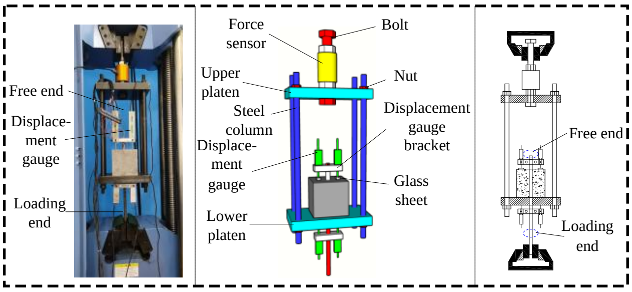

Fig. 1. Loading device

3. ANALYSIS OF TEST RESULTS

The failure mode of the specimen is a pull-out failure, the surface of the pull-out failure specimen is complete, no cracks are found, and the steel bar at the loading end is pulled out about 25 mm in the loading direction, as shown in Fig. 2. The load-slip curve of the specimen is shown in Fig. 3. It can be seen that the pull-out failure is divided into an ascending section, a descending section and a residual section. Rising section: $0<s\leq su$ force and displacement slowly increase, and the force reaches a certain value (about 8.7 kN), At this stage, the chemical cementation force works; then the slope gradually decreases, the displacement increases speed becomes faster, the force increases speed slows down, and the force reaches the peak load, this stage is the mechanical bite force works. Descent section: $su<s\leq sr$, the force decreases rapidly, the displacement increases rapidly, and this stage is the combined effect of residual mechanical bite force and friction force. Residual section: s＞sr, the bonding stress-slip curve changes smoothly, the load remains unchanged, and enters the residual section, at this stage, only friction works.

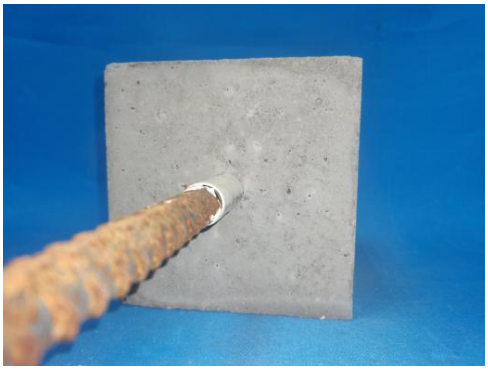

Fig. 2. Pull out damage

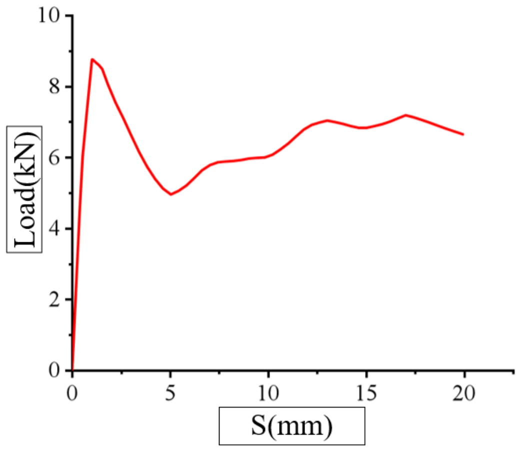

Fig. 3. Load-slip curve

4. FINITE ELEMENT SIMULATION

4.1 Create Part and Attribute Definitions

In this article, three parts are created: the concrete part, the steel part and the PVC pipe part. The sample is a cube with a side length of 150mm, the rebar has a diameter of 8 mm and a length of 200 mm, the inner diameter of the PVC pipe is the same as the steel bar, the outer diameter is 12mm, and the length of each section is 40mm. The three parts all use three-dimensional 8-node solid elements, and the element type is C3D8R. An important part of the definition of material properties is the selection of the material's tensile and compressive constitutive models. The constitutive model of the reinforcement adopts the ideal elastoplastic double-line model suggested in the 《Code for Design of Concrete Structures》 (GB50010-2010) [10], and the recycled concrete constitutive model of the concrete constitutive model references [11,12]. The drawing of each component is shown in Fig. 4.

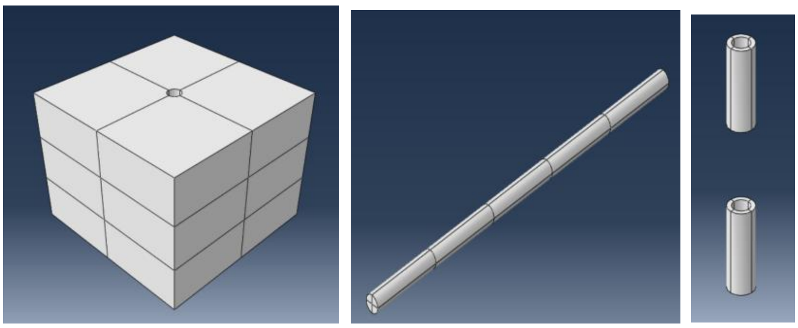

Fig. 4. Each part completes the graphics

4.2 Assembly

This step assembles the components established in the first step to form a complete specimen model. The operation is relatively simple, and the specimen is assembled through general commands such as translation, rotation, mirror image, and cutting. It is similar to the operation in available modelling software.

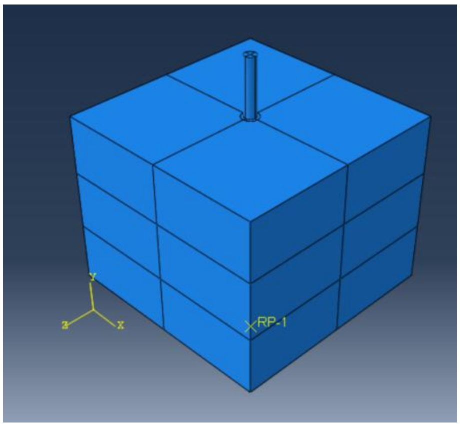

Fig. 5. Assembly Completed Drawing

4.3 Load Application and Analysis Step Setting

For this part of the test, the concrete specimens are mainly fixed and the displacement load is applied to the steel bars. Fig. 6 shows the completed load application.

Fixed constraints are applied to the concrete specimens, and after the surface of the steel bar is coupled, displacement loads are applied, mainly because the calculation results of displacement loading are easier to converge than force loading, so all the finite element simulations in this paper are carried out in the way of displacement loading.

Analysis step setting: This paper uses ABAQUS/CAE analysis step to solve. In order to better simulate the experiment, in addition to the initial analysis step, two analysis steps Step-1 and Step-2 need to be created. In the initial analysis step, the concrete part is fully fixed, and its translation and rotation are restricted until the end of loading, ie U1=U2=U3=UR1=UR2=UR3=0. In Step-1, the free end of the steel bar is completely fixed, and the loading end is given a displacement along the force direction U2, whose magnitude is the deformation of the steel bar, and the translation and rotation in the other directions are restricted. In Step-2, the constraint of the free end of the steel bar along the load direction U2 is released, and the displacement of the loaded end of the steel bar is modified to be the slip value measured in the test. In addition, since the slip of reinforced concrete belongs to nonlinear analysis, check the geometric nonlinear switch in the analysis step settings.

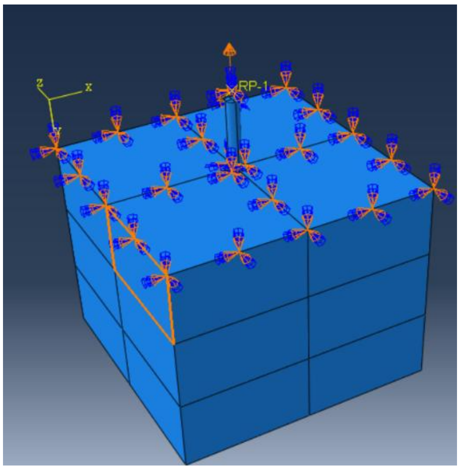

Fig. 6. Applied load completion diagram

4.4 Meshing

For component meshing, too large meshing may easily lead to insufficient calculation accuracy, and too dense meshing may easily lead to long calculation time and difficulty in convergence. In addition to the above factors, it is also necessary to ensure that the concrete element mesh and the steel element mesh have the same node, to set the nonlinear spring element accurately. Therefore, we divide the grid size of concrete, steel bars and PVC pipe elements into 5 mm, as shown in Fig. 7.

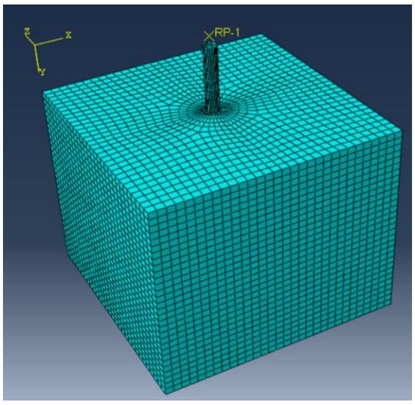

Fig. 7. Schematic diagram of mesh division

4.5 Nonlinear Spring Element

The setting of the spring element is the key to the establishment of the finite element model in this paper. In order to verify the accuracy of the test, this paper uses the nonlinear spring element Spring-2 to simulate the bond-slip between steel and concrete. Since only linear springs can be defined in the pre-processing of ABAQUS software, it is necessary to generate an INP file first, and then modify the linear spring in the INP file to a nonlinear spring. INP file redefined for non-linear spring Spring-2. To establish a nonlinear spring unit, the FD curve must first be confirmed based on the experimental data. The FD curve is based on the load-slip curve of the existing experiment, divided by the number of nonlinear spring units to be generated, and the properties of each group of nonlinear spring units can be defined.

After obtaining the F-D curve data, modify the linear spring part in the INP file to a nonlinear spring. The process is as follows:

Find the relevant statements of the spring unit in the INP file:

①*Spring, elset=Springs/Dashpots-1-spring
……
*Element,type=SpringA,elset=Springs/Dashpots-1-spring
……
Change the content in ① to the following:
*Spring, elset=Springs/Dashpots-1-spring, NONLINEAR
2, 2
-15.09340154,-20
-15.30780738,-19.5
-15.52228414,-19
……
*Element, type=Spring2, elset=Springs/Dashpots-1-spring
1,Steel-bar-1.2,final-concrete-1.11
2,Steel-bar-1.3,final-concrete-1.

Adding NONLINEAR after the *Spring, elset=Springs/Dashpots-1-spring statement means changing the linear spring to a nonlinear spring. 2, 2 represents the direction of the defined spring, that is, the force direction Y direction in this paper. The data below represent the F-D curves obtained from the test results. And 1, Steel-bar-1.2, and final-concrete-1.11 represent the two parts connected by the spring and their node numbers.

4.6 Comparison of Postprocessing Results

Figs. 8 and 9 illustrate the Mises stress cloud diagrams of bonded specimens. It can be seen from the figure that the Mises stress distribution of concrete radiates to the surrounding area along the bonded area and gradually decreases, and the Mises stress distribution of steel bars in the bonded section The law is gradually decreasing from the loading end to the free end, which is consistent with the test results and proves the validity of the finite element simulation results. And the accuracy of the nonlinear spring element method can be seen from the comparison of the test and finite element result curves in Fig. 10. Fig. 11 shows the distribution of bond stress along the anchorage length, which is similar to the general test. The stress increases first and then decreases, and peaks near the loading end.

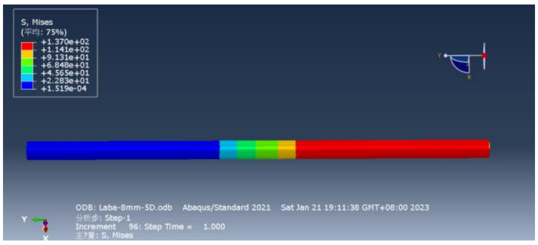

Fig.8. Reinforcement stress cloud diagram

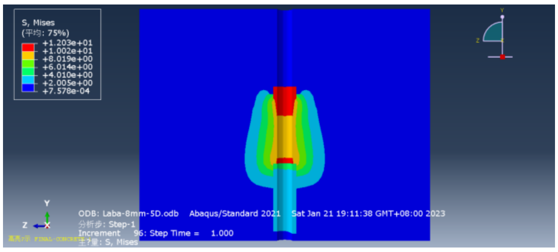

Fig.9. Concrete stress cloud diagram

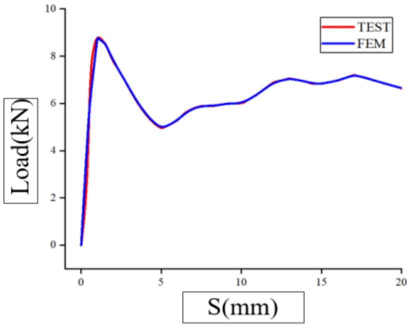

Fig.10. Comparison of test and finite element results

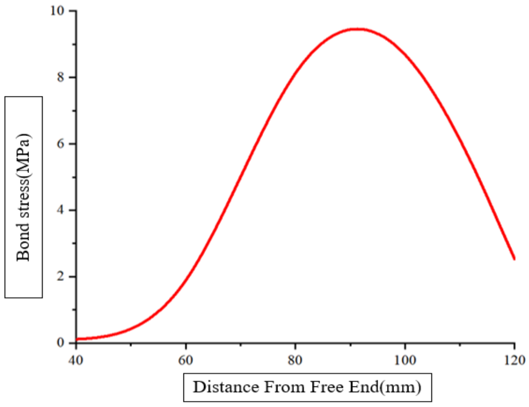

Fig.11. Bond stress distribution along the anchorage length

5. CONCLUSION

1) From the load-slip curve of the specimen, it can be seen that the failure mode of the pull-out test is divided into ascending section, descending section and residual section. This is consistent with the failure mode of most RC-bonded specimens.
2) In the bond test of recycled aggregate concrete, the strain curve of steel bars is convex. In general, the strain of reinforcement is small near the loading end and the free end, and steep in the middle.
3) The finite element simulation analysis results of the central pull-out experiment of steel bars and recycled concrete are consistent with the test results, which shows that the nonlinear spring element method is accurate and proves the effectiveness of the finite element simulation results. It provides a more accurate scheme for extracting the bond stress between steel bars and recycled concrete.

ACKNOWLEDGEMENTS

The authors gratefully acknowledge the support from the National College Students' Innovation and Entrepreneurship Training Program in Henan Province in 2022 (202210485010) the Science and Technology Department of Henan Province (222102320116, 212102310973).

COMPETING INTERESTS

Authors have declared that no competing interests exist.

REFERENCES

1. Cheng DH, He GY, Sun CH. Analysis of anchorage performance of reinforced recycled concrete. Shanxi Architecture. 2017;43(29):54-55.
2. Cao WL, Lin DC, Qiao QY, et al. Study on the bonding properties and influencing factors of steel bar and recycled concrete. Journal of Natural Disasters. 2017; 26(5):36-44.
3. Hu Q, Chen WW, Zou YC. Experimental study on bonding properties of recycled concrete. Journal of Harbin Institute of Technology. 2010;42(12): 1849-1854.
4. Wang CX, Wu J, Chen ZH. Experimental study on the bond-slip performance of steel bars and recycled concrete. Journal of Civil Engineering. 2013;46(S2): 225-231.
5. Li PC, Peng YK, Li F, et al. Effect of recycled coarse aggregate on bonding properties of reinforced concrete. Civil Architecture and Environmental Engineering. 2016;(s1).
6. Xiao J Z, Li P S, Qin W. Bond-slip behavior between recycled concrete and steel bars. Journal of Tongji University (Natural Science Edition). 2006;34(1): 13-16.
7. Abbas H, Elsanadedy H, Alaoud L, Almusallam T, Al-Salloum Y. Effect of confining stirrups and bar gap in improving bond behavior of glass fiber reinforced polymer (GFRP) bar lap splices in RC beams. CONSTR BUILD MATER. 2023; 365129943.
8. Lv M, Gao D, Yang L, Li C, Tang J. Bond properties between concrete and high ductility cementitious composite with totally recycled fine aggregate. Constr build mater. 2022; 357129373.
9. Chen YS, Zeng SH, Dong FZ, et al. Experimental study on the bond stress distribution of deformed reinforcement in lightweight aggregate concrete. Building Structure. 2006;34(1): 13-16.
10. Shen PS. New Code for design of concrete structures (GB50010-2010). Mechanical Industry Press.

11. Xiao JZ. Uniaxial compressive stress-strain full curve test research on recycled concrete. Journal of Tongji University (Natural Science Edition). 2007;(11):1445-1449.

12. Xiao JZ, Lan Y. Experimental study on uniaxial tensile performance of recycled concrete. Journal of Building Materials. 2006;(02): 154-158.

Peer-review history:
The peer review history for this paper can be accessed here:
https://www.sdiarticle5.com/review-history/98153